OCEAN MICROBIOLOGY

Metagenomic analysis reveals global-scale patterns of ocean nutrient limitation

Lucas J. Ustick[1]†, Alyse A. Larkin[2]†, Catherine A. Garcia[2], Nathan S. Garcia[2], Melissa L. Brock[1], Jenna A. Lee[2], Nicola A. Wiseman[2], J. Keith Moore[2], Adam C. Martiny[1,2]*

Nutrient supply regulates the activity of phytoplankton, but the global biogeography of nutrient limitation and co-limitation is poorly understood. *Prochlorococcus* adapt to local environments by gene gains and losses, and we used genomic changes as an indicator of adaptation to nutrient stress. We collected metagenomes from all major ocean regions as part of the Global Ocean Ship-based Hydrographic Investigations Program (Bio-GO-SHIP) and quantified shifts in genes involved in nitrogen, phosphorus, and iron assimilation. We found regional transitions in stress type and severity as well as widespread co-stress. *Prochlorococcus* stress genes, bottle experiments, and Earth system model predictions were correlated. We propose that the biogeography of multinutrient stress is stoichiometrically linked by controls on nitrogen fixation. Our omics-based description of phytoplankton resource use provides a nuanced and highly resolved description of nutrient stress in the global ocean.

The supply of nutrients to the surface ocean exerts a fundamental control on phytoplankton growth (*1*) that may be further exacerbated by future climate-driven stratification (*2*). However, there is currently large uncertainty about the global patterns of nutrient stress and the possibility of limitation by multiple nutrients (*3*). For example, studies have independently proposed N, P, or Fe limitation for phytoplankton growing in the North Atlantic Ocean (*4*–*6*). Thus, the role and interactions of each nutrient in regulating phytoplankton growth is still unknown for large parts of the ocean.

Experimental nutrient additions and biogeochemical models are important tools for quantifying ocean nutrient stress (*7*). Nutrient additions have demonstrated Fe limitation in upwelling regions, but it has been difficult to identify the limiting nutrient in many other places. Multiple elements are often required to stimulate growth (*8*), leading to a proposal of widespread co-limitation (*7*). However, nutrients are commonly present simultaneously at low concentrations, making it challenging to distinguish between co-limitation and the quick exhaustion of nonlimiting nutrients (*9*). Bottle experiments can also introduce artifacts and are labor intensive, leading to large regional gaps in coverage (e.g., most of the Indian Ocean) (*7*). Ocean biogeochemical models predict large-scale patterns of nutrient limitation. However, the degree of nutrient stress and the boundaries between major nutrient-limitation regimes are sensitive to uncertain descriptions of uptake and growth as well as external nutrient inputs (*10*). Thus, there are methodological and conceptual challenges associated with quantifying the biogeography of ocean nutrient stress.

Prochlorococcus, the most abundant phytoplankton in oligotrophic regions (*11*), can adapt to low-nutrient conditions through gene gains and losses. The fast growth and large population size of *Prochlorococcus* results in a close association between genome content and local nutritional conditions (*11*). All *Prochlorococcus* genomes include the *pstABCS* genes for direct assimilation of available inorganic phosphate (*12*, *13*). However, cells gain the capacity for regulation (e.g., *phoBR*) and assimilation of specific P-containing compounds when inorganic P is depleted. They also detoxify the accidental uptake of arsenate with *arsR/acr3* (*14*). Under high P depletion and stress, cells can broadly assimilate dissolved organic P (DOP) using the alkaline phosphatases *phoA* and *phoX* (*15*, *16*). A similar phylogenomic hierarchy of adaptation is seen for N and Fe acquisition and stress. *Prochlorococcus* cells progressively gain the capacity for ammonia, urea, nitrite, and nitrate uptake with increasing N stress driven by energetic costs of converting oxidized N compounds into glutamine (*17*, *18*). *Prochlorococcus* cells carry genes for increasing uptake by siderophores and additional transporters under medium Fe stress (*19*) and have lost many Fe-containing proteins under severe Fe stress in high-nutrient, low-chlorophyll (HNLC) zones (*20*). Thus, genomic content of cells in a region reflects the experienced physiological nutrient stress and the biochemical tradeoffs in overcoming the severity of nutrient stress by loss of function or investments in acquisition (*21*). Thus, we propose using the genome content of *Prochlorococcus* populations as a global-scale biosensor for ocean phytoplankton nutrient stress.

We collected surface metagenomes from the Atlantic, Pacific, and Indian Oceans to quantify the global genome content of *Prochlorococcus* and inferred nutrient stress (table S1 and data S1). A total of 909 samples were newly collected as part of the Global Ocean Ship-based Hydrographic Investigations Program (Bio-GO-SHIP) (*22*) and supplemented with 228 from Tara Oceans (https://oceans.taraexpeditions.org/) and GEOTRACES (https://www.geotraces.org/). We recruited sequences to known *Prochlorococcus* strains, recorded the frequency of established nutrient acquisition genes, and normalized to *Prochlorococcus* single-copy core genes. On the basis of prior biochemical knowledge and as verified by phylogenomics (and without reference to their spatial distribution), we a priori classified genetic adaptations for overcoming a nutrient stress type and severity (Ω) (Table 1 and data S2). Although the classification of adaptations into high, medium, and low stress partially masks the complex biochemical tradeoffs and phylogenomic trait hierarchy of nutrient use, these groupings allow us to quantify the geographic variation of nutrient stress environments in the global surface ocean.

Table 1. *Prochlorococcus* genes associated with nutrient stress type and severity.

$\Omega_{type,severity}$	Function	Marker genes	Reference(s)
$\Omega_{Fe,high}$	Loss of Fe-containing proteins	HLIII-IV core genes	(*20*)
$\Omega_{Fe,medium}$	Fe uptake (transporters)	*cirA*, *expD*, *febB*, *fepB/C*, *tolQ*, *tonB*	(*19*)
$\Omega_{P,high}$	Alkaline phosphatase	*phoA*, *phoX*	(*12*, *15*)
$\Omega_{P,medium}$	P starvation regulation, arsenate toxicity, specific DOP assimilation	*arsR*, *acr3*, *chrA*, *gap1*, *mfs*, *phoB/E/R*, *ptrA*, *PMM707*, *PMM721*, *unkP1-5*	(*12*–*14*)
$\Omega_{N,high}$	Nitrite and nitrate assimilation and uptake	*focA*, *moaA-E*, *moeA*, *napA*, *narB*, *nirA*	(*17*)
$\Omega_{N,medium}$	Urea and cyanate utilization	*cynA/S*, *tauE*, *ureA-G*, *urtA*, *unkN1-2*	(*17*, *18*)

[1]Department of Ecology and Evolutionary Biology, University of California Irvine, Irvine, CA 92697, USA. [2]Department of Earth System Science, University of California Irvine, Irvine, CA 92697, USA.
*Corresponding author. Email: amartiny@uci.edu
†These authors contributed equally to this work.

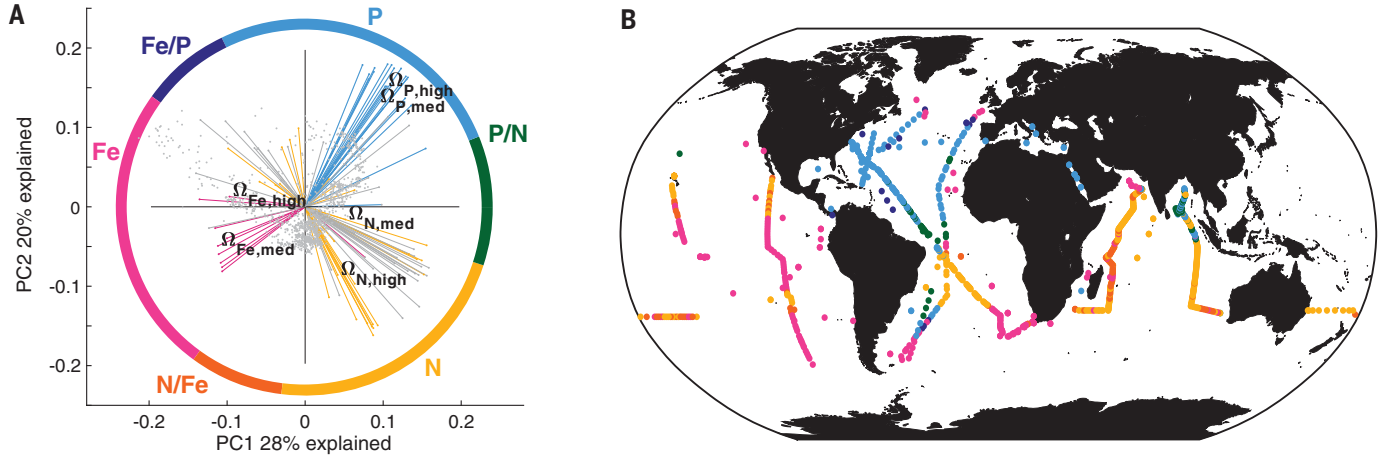

Fig. 1. Variation in nutrient stress genes among *Prochlorococcus* populations. (**A**) Principal component analysis of stress genes across all metagenome samples (gray dots, n = 1137). Vectors for stress genes (z_i) and composite metrics (Ω_s) are overlaid and colored according to nutrient type: red, Fe; blue, P; yellow, N; and gray, low stress. The outer ring represents angular separation and the boundaries at which samples are categorized by nutrient stress type (table S2). (**B**) Global biogeography of nutrient stress type defined by the angular separation in (A).

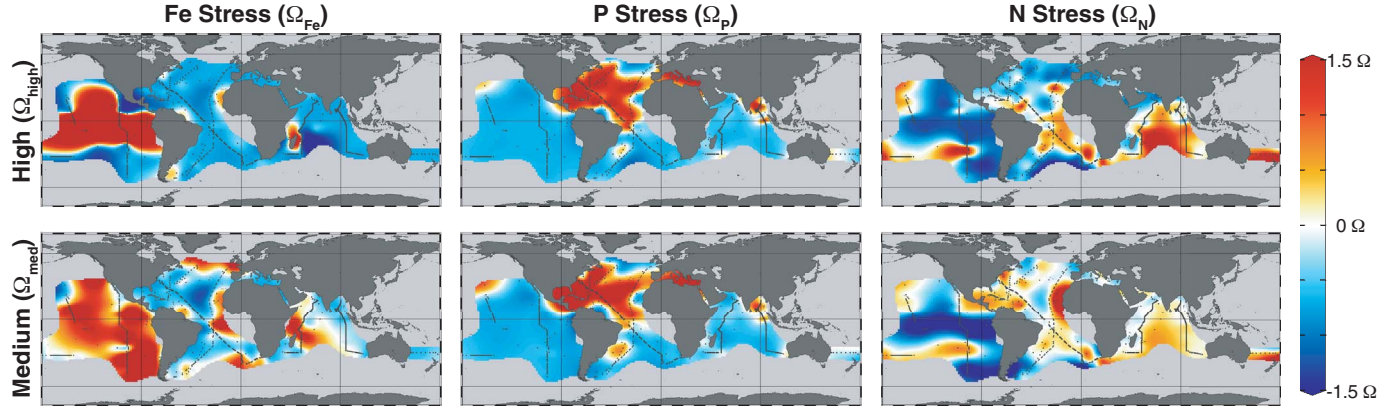

Fig. 2. Global biogeography of *Prochlorococcus* nutrient stress type and severity. On the basis of their biochemical role, genes were categorized by nutrient stress "type" and "severity" and combined into a composite metric (Ω_s) (Table 1). Background coloring is based on an interpolation between sampling points shown in dark gray.

An ordination of nutrient genes demonstrated a continuum of stress type and severity (Fig. 1A and fig. S1). The first principal component (28% variance) was parallel to the occurrence of medium- and high-N-stress indicator genes, suggesting that the largest cluster of samples was linked to N stress. The second principal component (20% variance) separated Fe and P stress genes, and the vectors for Fe and P stress genes pointed in nearly opposite directions (0.9π angular difference). There was also a spread within the N cluster related to N substrate (fig. S2). The vectors for populations with only ammonia and urea assimilation genes had nearly the same angle but were separated by 0.33π from populations containing nitrite + nitrate or cyanate genes (fig. S1). We propose that these samples were associated with medium versus high N stress. Several low-light strains of *Prochlorococcus* can use nitrite but not nitrate with a dedicated transporter *focA*. The *focA* and *narB* vectors were nearly in opposite directions (separated by 0.88π), suggesting a distinct ecological niche for nitrite assimilation (cooler waters with deeper mixing; figs. S1 and S2). Samples associated with elevated medium- and high-P-stress genes were predominantly from the North Atlantic Ocean and Mediterranean Sea, where high P stress has been proposed (*6*) (Fig. 1B). Samples associated with the high-Fe-stress genotype were mostly from the HNLC regions. However, selection for medium-stress genes occurred in many samples, suggesting widespread adaptation to Fe stress. We identified sample clusters between the N and Fe as well as the N and P gene vectors indicating frequent co-stress. By contrast, Fe and P stress genes showed low correlation (fig. S3) and there were rare co-occurrences of Fe-P stress genes. In sum, the ordination of *Prochlorococcus* genes could identify samples with genes linked to single-nutrient stress or co-stress.

Prochlorococcus genome content confirmed known biogeographic patterns but also revealed several previously unrecognized regions of nutrient (co-)stress (Fig. 1B). We observed genotypes adapted to (i) widespread N stress in oligotrophic regions; (ii) P stress in the North Atlantic Ocean, Mediterranean Sea, and Red Sea; and (iii) Fe stress in the equatorial Pacific Ocean. We found additional smaller regions of P stress adaptation in the western South Atlantic Ocean and the North Indian Ocean. Other regions with Fe stress adaptation included the eastern South Pacific Subtropical Gyre, temperate regions in the North and

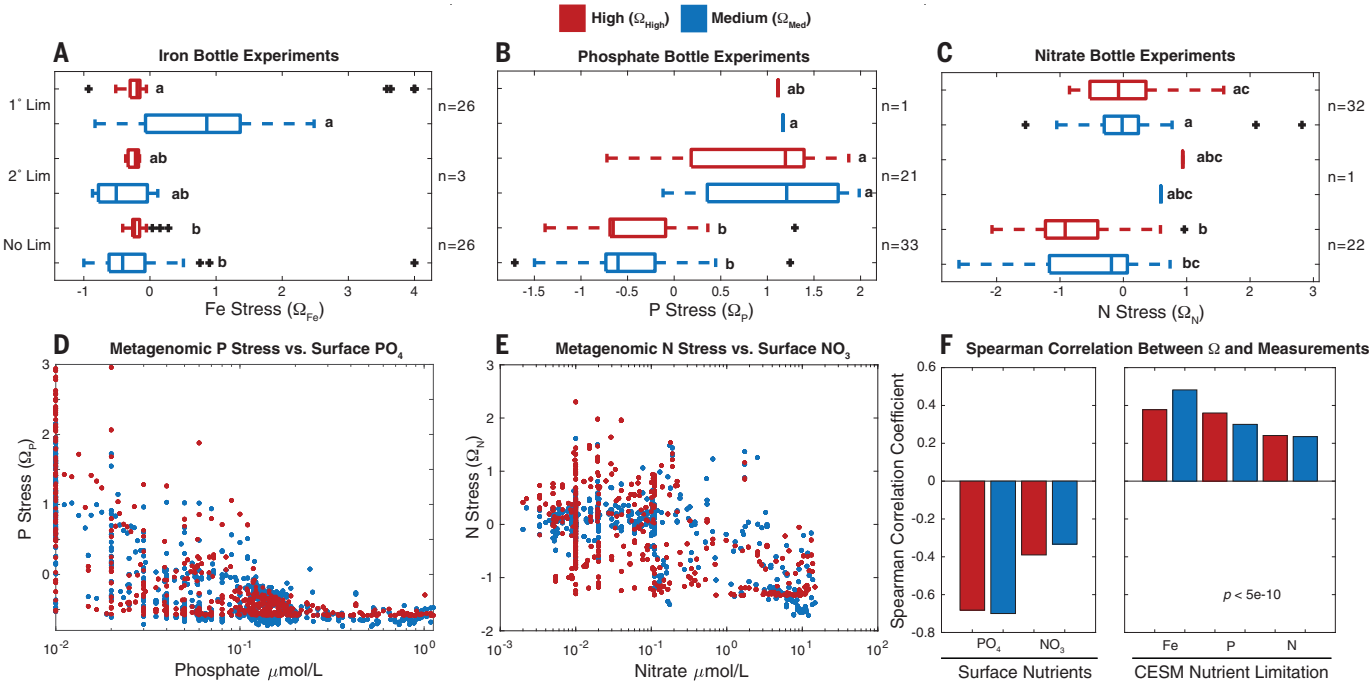

Fig. 3. Comparison between the *Prochlorococcus* biosensor and established approaches to characterizing nutrient stress. (**A**) Comparison between Fe addition experiments and genomic Fe stress (Ω_{Fe}) (n = 55). (**B**) Comparison between P addition experiments and genomic P stress (Ω_P) (n = 55). (**C**) Comparison between N addition experiments and genomic N stress (Ω_N) (n = 55). Small letters in (A) to (C) represent a Tukey post hoc comparison. (**D**) Comparison between surface phosphate concentrations and Ω_P (n = 658). (**E**) Comparison between surface nitrate concentrations and Ω_N (n = 802). (**F**) Summary of Spearman correlations between established approaches and genomic stress (Ω_S). All correlations are significant ($p < 5 \times 10^{-10}$). Data are colored by stress level across all figures (red, high-stress Ω_{High}; blue, medium-stress Ω_{Med}).

South Atlantic Ocean, and the Arabian Sea. Our data suggested that co-stress was widespread but mostly included N as one of the elements.

Prochlorococcus stress genes demonstrated subtle transitions between nutrient stress type and severity in the Atlantic Ocean (Fig. 2 and figs. S4 to S7 and S13). Samples from three independent ocean transects detected a transition between elevated Ω_{Fe} and Ω_P moving from north to south around 40° to 50°N (figs. S4 to S7). Subtle Fe stress north of the Gulf Stream has been observed in past physiological analyses of phytoplankton (*23*). Genes for DOP utilization and associated $\Omega_{P,high}$ >1 were observed in the North Atlantic subtropical gyre between ~40°N and the Intertropical Convergence Zone (ITCZ) but peaked near 30°N (figs. S4 to S7). An exception was a smaller region of elevated $\Omega_{Fe,med}$ in the Canary Current, where upwelling likely relieved macronutrient stress. In the central-eastern gyre core, we detected $\Omega_{N,high}$ >1, suggesting adaptation to N-P co-limitation. Some samples from the western gyre showed an unusual combination of co-occurring Fe-P stress genes. A clear meridional shift between P stress and other nutrients at the ITCZ has been suggested (*24*). In support, $\Omega_{P,high}$ and $\Omega_{P,med}$ were substantially lower in the South Atlantic Ocean ($\Omega_{P,high}$ = −0.5 to 0.5, $\Omega_{P,med}$ = −0.5 to 1) and constrained to a small western gyre region. By contrast, genotypes in the eastern South Atlantic Ocean indicated adaptation to medium Fe stress ($\Omega_{Fe,med}$ = 1 to 1.5). This is consistent with recent bottle experiments (*8*) as well as a negative east-west gradient in P concentration (*25*). $\Omega_{N,high}$ was positive in the central part of the South Atlantic subtropical gyre ($\Omega_{N,high}$ = 0.5 to 1), indicating strong N stress in the region (figs. S4 to S7). In parallel to the north, $\Omega_{Fe,med}$ rose near the subtropical front toward the Southern Ocean. Distinct nutritional regimes are thus present across the Atlantic Ocean.

The Pacific Ocean also showed clear transitions in stress type and severity. We detected a sharply bounded region in the eastern equatorial Pacific Ocean with $\Omega_{Fe,high}$ >1 (figs. S8, S9, and S13). There was also a surrounding zone with elevated $\Omega_{Fe,med}$, revealing a wider impact of upwelling on Fe stress than indicated by macronutrient concentrations (figs. S8 and S9). To the north of the HNLC region, $\Omega_{Fe,med}$ was eventually replaced with elevated $\Omega_{N,high}$ ($\Omega_{N,high}$ = 0.5, $\Omega_{Fe,med}$ = 0) and some P stress genes near Station ALOHA (http://aco-ssds.soest.hawaii.edu/ALOHA/). $\Omega_{Fe,med}$ was >1 in most of the southeastern Pacific Ocean, which is consistent with Fe stress seen in bottle incubations and photophysiology studies (*26*, *27*). There was additional elevated $\Omega_{N,high}$ in the South Pacific Ocean gyre core surrounded by a wider zone with high $\Omega_{N,med}$ (fig. S9). In the western South Pacific Ocean, we mainly detected adaptation to N stress ($\Omega_{N,high}$ = 0.5 to 1.5, $\Omega_{N,med}$ = 0.5 to 1) (fig. S10). However, there were slight increases in Ω_P toward the western edge of the gyre ($\Omega_{P,high}$ = 0 to 0.5, $\Omega_{P,med}$ = 0 to 0.2) (fig. S10). This zonal shift toward increasing P stress was consistent with the low P concentrations in the southwestern Pacific Ocean (*25*). We lacked samples from large regions of the Pacific Ocean (including the northwest), illustrating the substantial effort required to cover the entire Pacific basin.

We previously had a limited understanding of nutrient stress in the Indian Ocean (*7*, *28*), but two recent Global Ocean Ship-based Hydrographic Investigations Program (GO-SHIP; https://www.go-ship.org/) expeditions greatly improved metagenomics coverage. Most of the Indian Ocean had elevated $\Omega_{N,high}$ and $\Omega_{N,med}$ (figs. S11 to S13), with the highest values seen in the Southern Indian Ocean gyre. N stress genes decreased north of the equator and were lowest in the Arabian Sea upwelling region (figs. S11 and S13). We detected a region with elevated $\Omega_{P,high}$ on the northeastern side of the Indian Ocean associated with several

fronts from the equator to the Bay of Bengal (fig. S12). There were also indications of some P stress adaptation associated with the south-flowing Leeuwin and Agulhas currents. Samples from GO-SHIP I07N (fig. S11) ($\Omega_{Fe,high}$ = 0.5, $\Omega_{Fe,med}$ = 1 to 2) and Tara Ocean (fig. S13) ($\Omega_{Fe,high}$ = 3, $\Omega_{Fe,med}$ = 1) both demonstrated high Ω_{Fe} in a small upwelling region near 10°S on the western side of the basin. This zone of high Ω_{Fe} is supported by satellite and model studies (*29*). There was also widespread elevated $\Omega_{Fe,med}$ in most of South Indian Ocean gyre and in a few samples in the Arabian Sea (*30*). Overall, our metagenomics assessment greatly expands our understanding of nutrient stress across the Indian Ocean basin.

We speculate that the global-scale biogeography of *Prochlorococcus* multinutrient adaptation is stoichiometrically linked by N fixation. *Prochlorococcus* can use nutrients at a stoichiometric ratio substantially above the vertically supplied N:P (*31*). This leads to a default state of residual phosphate and corresponding N limitation in oligotrophic regions unless additional N is supplied by diazotrophs (*32*). As reflected in the relative ordination positions in Fig. 1A, cells appear to become adapted to simultaneous N-Fe co-stress if the external Fe supply and diazotroph activity are low. Moving counterclockwise in Fig. 1A, populations are mainly N stressed at an intermediate Fe supply, and then ultimately P stressed at high Fe supply and N fixation rates (*33*). The Atlantic meridional shift in nutrient stress emerges from these stoichiometric interactions (*34*). We saw signs of the same connections in the zonal shifts from elevated $\Omega_{Fe,med}$ in the southeastern Atlantic and Pacific Oceans toward elevated $\Omega_{P,med}$ and $\Omega_{P,high}$ in the southwestern Atlantic and Pacific Oceans. Cellular resource demand results in adaptation to high Fe stress in the upwelling zone in the equatorial Pacific Ocean (*35*). As the water flows outward, cells experience and adapt to first medium Fe/N, and then high N stress and even some P stress near Station Aloha as the vertical Fe:P supply ratio increases. These meridional and zonal shifts in adaptation to nutrient stress mirror a recent synthesis of surface phosphate concentrations (*25*). An exception was the North Indian Ocean and Bay of Bengal, where we detected a region of high Ω_P without a clear connection to N fixation (*36*). We detected samples with Fe-P co-stress in the western North Atlantic Ocean. Because Fe and P stress are commonly opposite (Fig. 1A), this co-stress may be linked to the lateral advection of low-P water from the central Atlantic Ocean (*37*). Despite the exceptions, our omics-based approach supports an emergent stoichiometric connection of oceanic multinutrient stress.

We saw a significant correspondence between *Prochlorococcus* stress genes and nutrient addition experiments, Earth system model predictions, and the depletion of surface nutrient concentrations (Fig. 3). There was a significant increase in the frequency of *Prochlorococcus* stress genes from no limitation, to co-limitation (2°), and then to primary (1°) limitation using bottle experiments (Fig. 3, A to C) (*7*). However, there was no distinction between medium and high stress and bottle experiments.

There were also significant negative correlations between Ω_P and Ω_N and surface phosphate or nitrate concentrations, respectively (Fig. 3, D to F). At high phosphate concentrations, Ω_P was depressed, but a wide range in Ω_P appeared at low phosphate concentrations (Fig. 3D). There was also a significant correlation between Ω_N and nitrate concentrations, but again with a considerable spread (Fig. 3E). This pattern suggested a large spread in stress among *Prochlorococcus* populations at low nutrient concentration that could be driven by stoichiometric interactions with other nutrients or shifts in the supply rate of nutrients to the surface ocean. We saw a limited difference between Ω_{med} and Ω_{high} and the respective nutrient concentration. Thus, the metagenomic approach can delineate stress even when nutrients are severely depleted.

There was a broad agreement between Ω and simulated nutrient stress in an Earth system model [CESMv2_BEC (*38*)] (Fig. 3F and fig. S14). The strongest overlap in Fe stress was observed in the eastern equatorial Pacific Ocean. However, Ω_{Fe} suggested additional adaptation to Fe stress in the eastern Pacific Ocean, the southeastern Atlantic Ocean, and the south-central Indian Ocean (fig. S14), all regions where the biogeochemical model predicted N stress. This is at least partially a CESMv2_BEC bias, because both satellite and other model data support severe Fe stress in the Indian Ocean region (*29*), and recent incubation experiments found some Fe stress in the southeastern Atlantic Ocean (*3*). CESMv2_BEC and Ω_P agreed on P stress in the western North Atlantic Ocean, but Ω_P suggested adaptation to P stress in the wider subtropical North Atlantic Ocean. Both efforts detected a smaller P stress region in the southwestern Atlantic Ocean. However, CESMv2_BEC did not show any P stress in the northern Indian Ocean. There was broad agreement between CESMv2_BEC and Ω_N throughout most of the Pacific and Atlantic Oceans. However, Ω_N suggested stronger N stress adaptation in the Indian Ocean than captured in CESMv2_BEC. With the exception of the little-studied Indian Ocean, there was broad agreement in the regional patterns of nutrient stress between an Earth system model and our omics-based metric.

There are several important caveats to consider. First, genomic variations can reflect both the demand for nutrients as well as the availability of different nutrient species. Cyanobacteria up-regulate the acquisition of oxidized N sources at a low ammonia supply and have no dedicated sensory proteins for the concentration of urea or nitrate (*39*). In addition, the genome organization of N acquisition supports sequential acquisition of ammonia, urea, nitrite, and nitrate genes (fig. S15) (*40*). For example, as illustrated by our eastern Pacific Ocean transect, there was strong upwelling and divergent flow of nitrate centered on 5°S (fig. S16). At the upwelling core with high nitrate, *Prochlorococcus* solely contained genes for ammonia uptake and thus likely relies on recycled ammonia, followed by urea at the gyre transition (~15°S), and then nitrate assimilation within the gyre (~30°S). Moreover, there was an inverse relationship between surface nitrate concentrations and nitrate reductase in *Prochlorococcus*. Thus, the genome regulation, genome organization, and biogeography of *Prochlorococcus* nutrient acquisition genes suggest a first-order relationship with cellular resource demands and environmental gradients in nutrient availability, and thus an experienced stressful supply. However, it appears unlikely that cells would retain these genes without access to the associated resources being supplied by community recycling (e.g., through nitrification). Second, we categorized a priori each gene into three levels of stress severity based on their biochemical role, phylogenomics, and regulation to avoid "circularity" in our quantification of nutrient stress. However, the biogeographic patterns suggest that nitrite assimilation occurs in regions with deep mixing and likely lower N stress, whereas cyanate utilization genes covary closely with high N stress. Furthermore, medium- and high-phosphate-stress genes generally co-occur, suggesting a limited resolution of regional P stress. Thus, some genes could be reclassified or added to the classification system (e.g., assimilation of organic N sources) (*41*) in future analyses to refine the approach. A third caveat is that our study is based on the assessment of nutrient stress adaptation in a single organism. *Prochlorococcus* is the smallest and most abundant phytoplankton in most nutrient-limited marine ecosystems between 40°N and 40°S (*11*). However, *Prochlorococcus* is not abundant or even present in many coastal or high-latitude environments, restricting the geographical reach of the technique. Furthermore, coexisting taxa could show divergent nutrient stress profiles because of physiological differences (*21*, *31*, *42*). However, *Prochlorococcus* generally has the highest nutrient uptake affinity and is least likely to experience cellular nutrient stress (*43*). We also found a significant correspondence between our stress metric and three established approaches, implying that we captured the general community physiological state in the regions analyzed. A fourth caveat is the use of genomic changes to assess

the underlying physiological state: A genome-based approach will work in populations with rapid adaptation to local conditions, but transcriptomic or proteomic approaches may work better in ecosystems with longer generation times. However, these approaches are more labor intensive and affected by strong diurnal expression changes. Thus, omics-based assessments of nutrient stress should be carefully calibrated to the biological behavior of the targeted ecosystem.

Connecting omics-based microbiome studies and biogeochemically important processes is a widespread convergence challenge, and links have been elusive and mainly correlation based (*44*). Our stress metric builds upon 30 years of studies of *Prochlorococcus* physiology and adaptation to different nutrient regimes and allows for a mechanistic description of resource utilization. It is also a semiquantitative, cost-effective, and standardized way of assessing nutrient stress and does not require labor-intensive incubation experiments. Finally, our method can provide a sensitive description of phytoplankton stress and identify nutrient stress severity for multiple elements simultaneously (*9*). Thus, our findings demonstrate how we can harness omics-based information to develop a nuanced and high-resolution understanding of global biogeochemistry.

REFERENCES AND NOTES

1. T. Tyrrell, *Nature* **400**, 525–531 (1999).
2. L. Bopp *et al.*, *Biogeosciences* **10**, 6225–6245 (2013).
3. T. J. Browning *et al.*, *Nature* **551**, 242–246 (2017).
4. J. H. Martin, S. E. Fitzwater, R. Michael Gordon, C. N. Hunter, S. J. Tanner, *Deep. Res. Part II* **40**, 115–134 (1993).
5. M. Davey *et al.*, *Limnol. Oceanogr.* **53**, 1722–1733 (2008).
6. J. W. Ammerman, R. R. Hood, D. A. Case, J. B. Cotner, *Eos* **84**, 165–170 (2003).
7. C. M. Moore *et al.*, *Nat. Geosci.* **6**, 701–710 (2013).
8. T. J. Browning *et al.*, *Nat. Commun.* **8**, 15465 (2017).
9. E. A. Davidson, R. W. Howarth, *Nature* **449**, 1000–1001 (2007).
10. A. Krishnamurthy, J. K. Moore, N. Mahowald, C. Luo, C. S. Zender, *J. Geophys. Res.* **115**, G01006 (2010).
11. F. Partensky, L. Garczarek, *Ann. Rev. Mar. Sci.* **2**, 305–331 (2010).
12. A. C. Martiny, M. L. Coleman, S. W. Chisholm, *Proc. Natl. Acad. Sci. U.S.A.* **103**, 12552–12557 (2006).
13. D. J. Scanlan, N. J. West, *FEMS Microbiol. Ecol.* **40**, 1–12 (2002).
14. J. K. Saunders, G. Rocap, *ISME J.* **10**, 197–209 (2016).
15. S. Kathuria, A. C. Martiny, *Environ. Microbiol.* **13**, 74–83 (2011).
16. L. R. Moore, M. Ostrowski, D. J. Scanlan, K. Feren, T. Sweetsir, *Aquat. Microb. Ecol.* **39**, 257–269 (2005).
17. A. Herrero, A. M. Muro-Pastor, E. Flores, *J. Bacteriol.* **183**, 411–425 (2001).
18. A. C. Tolonen *et al.*, *Mol. Syst. Biol.* **2**, 53 (2006).
19. R. R. Malmstrom *et al.*, *ISME J.* **7**, 184–198 (2013).
20. D. B. Rusch, A. C. Martiny, C. L. Dupont, A. L. Halpern, J. C. Venter, *Proc. Natl. Acad. Sci. U.S.A.* **107**, 16184–16189 (2010).
21. C. A. Garcia *et al.*, *Philos. Trans. R. Soc. Lond. B Biol. Sci.* **375**, 20190254 (2020).
22. A. A. Larkin *et al.*, *Sci Data* **8**, 107 (2021).
23. M. C. Nielsdóttir, C. M. Moore, R. Sanders, D. J. Hinz, E. P. Achterberg, *Global Biogeochem. Cycles* **23**, GB3001 (2009).
24. R. L. Mather *et al.*, *Nat. Geosci.* **1**, 439–443 (2008).
25. A. C. Martiny *et al.*, *Sci. Adv.* **5**, eaax0341 (2019).
26. S. Bonnet *et al.*, *Biogeosciences* **5**, 215–225 (2008).
27. M. J. Behrenfeld, Z. S. Kolber, *Science* **283**, 840–843 (1999).
28. B. S. Twining *et al.*, *Deep. Res. Part II Top. Stud. Oceanogr.* **166**, 125–140 (2019).
29. M. J. Behrenfeld *et al.*, *Biogeosciences* **6**, 779–794 (2009).
30. S. W. A. Naqvi *et al.*, *Biogeosciences* **7**, 2091–2100 (2010).
31. A. R. Moreno, A. C. Martiny, *Ann. Rev. Mar. Sci.* **10**, 43–69 (2018).
32. M. M. Mills, K. R. Arrigo, *Nat. Geosci.* **3**, 412–416 (2010).
33. J. Wu, W. Sunda, E. A. Boyle, D. M. Karl, *Science* **289**, 759–762 (2000).
34. B. A. Ward, S. Dutkiewicz, C. M. Moore, M. J. Follows, *Limnol. Oceanogr.* **58**, 2059–2075 (2013).
35. M. A. Saito *et al.*, *Science* **345**, 1173–1177 (2014).
36. C. R. Löscher, W. Mohr, H. W. Bange, D. E. Canfield, *Biogeosciences* **17**, 851–864 (2020).
37. M. W. Lomas *et al.*, *Biogeosciences* **7**, 695–710 (2010).
38. J. K. Moore, S. C. Doney, K. Lindsay, *Global Biogeochem. Cycles* **18**, GB4028 (2004).
39. G. Rocap *et al.*, *Nature* **424**, 1042–1047 (2003).
40. A. C. Martiny, S. Kathuria, P. M. Berube, *Proc. Natl. Acad. Sci. U.S.A.* **106**, 10787–10792 (2009).
41. M. V. Zubkov, B. M. Fuchs, G. A. Tarran, P. H. Burkill, R. Amann, *Appl. Environ. Microbiol.* **69**, 1299–1304 (2003).
42. H. Alexander, B. D. Jenkins, T. A. Rynearson, S. T. Dyhrman, *Proc. Natl. Acad. Sci. U.S.A.* **112**, E2182–E2190 (2015).
43. M. W. Lomas, J. A. Bonachela, S. A. Levin, A. C. Martiny, *Proc. Natl. Acad. Sci. U.S.A.* **111**, 17540–17545 (2014).
44. J. D. Rocca *et al.*, *ISME J.* **9**, 1693–1699 (2015).

ACKNOWLEDGMENTS

We thank the chief scientists L. Barbaro, B. Carter, M. Lomas, R. Sonnerup, G. Tarran, and D. Volkov and the coordinators of GO-SHIP (L. Tally and G. Johnson) and the Atlantic Meridional Transect (AMT; A. Rees) for supporting the collection of metagenomic data. **Funding:** This work was supported by the National Science Foundation (OCE-1046297, 1559002, 1848576, and 1948842 to A.C.M. and 1658392 to J.K.M.), a National Aeronautics and Space Administration Earth and Space Science Fellowship (NESSF16R to C.A.G.), the National Institutes of Health (T32AI141346 to L.J.U.), and the DOE BER Earth System Modeling Program (DE-SC0016539 to J.K.M.). A.M.T. is funded by the UK Natural Environment Research Council through its National Capability Long-term Single Centre Science Programme, Climate Linked Atlantic Sector Science (NE/R015953/1). This study contributes to the international Integrated Marine Biosphere Research (IMBeR) project (AMT contribution #358). **Author contributions:** L.J.U., A.A.L., and A.C.M. designed the study and wrote the manuscript with input from all authors. A.A.L., C.A.G., N.S.G., and J.A.L. collected samples. A.A.L., C.A.G., M.L.B., and J.A.L. sequenced metagenomes. L.J.U. analyzed the data. N.A.W. and J.K.M. produced CESM BEC model outputs. A.C.M. supervised the study. **Competing interests:** The authors declare no competing interests. **Data and materials availability:** All data are available in the main text or the supplementary materials. Raw metagenomic reads are available through the National Center for Biotechnology Information Sequence Read Archive (BioProject ID PRJNA656268). Metadata are available through http://cchdo.ucsd.edu and BCO-DMO (project 2178). A complete description of all Bio-GO-SHIP metagenomes and associated metadata are available (*22*).

SUPPLEMENTARY MATERIALS

science.sciencemag.org/content/372/6539/287/suppl/DC1
Materials and Methods
Figs. S1 to S16
Tables S1 to S3
References (*45*–*61*)
Databases S1 and S2
MDAR Reproducibility Checklist

View/request a protocol for this paper from *Bio-protocol*.

10 September 2020; accepted 1 March 2021
10.1126/science.abe6301

Metagenomic analysis reveals global-scale patterns of ocean nutrient limitation

Lucas J. Ustick, Alyse A. Larkin, Catherine A. Garcia, Nathan S. Garcia, Melissa L. Brock, Jenna A. Lee, Nicola A. Wiseman, J. Keith Moore and Adam C. Martiny

Science **372** (6539), 287-291.
DOI: 10.1126/science.abe6301

Genomes reveal nutrient stress patterns

Within the surface ocean, nitrogen, iron, and phosphorous can all be limiting nutrients for phytoplankton depending on location. Ustick *et al.* used the prevalence of *Prochlorococcus* genes involved in nutrient acquisition to develop maps of inferred nutrient stress across the global ocean (see the Perspective by Coleman). They found broad patterns of limitation consistent with an Earth system model and nutrient addition experiments. Leveraging metagenomic data in this manner is an appealing approach that will help to expand our understanding of the biogeochemistry in the vast open ocean.

Science, this issue p. 287; see also p. 239

Science (print ISSN 0036-8075; online ISSN 1095-9203) is published by the American Association for the Advancement of Science, 1200 New York Avenue NW, Washington, DC 20005. The title *Science* is a registered trademark of AAAS.